Fuel 261 (2020) 116445

Contents lists available at ScienceDirect

Fuel

journal homepage: www.elsevier.com/locate/fuel

Full Length Article

AI based mechanistic modeling and probabilistic forecasting of hybrid low salinity chemical flooding

Cuong Dang[a,*], Long Nghiem[a], Eugene Fedutenko[a], Seyhan Emre Gorucu[a], Chaodong Yang[a], Arash Mirzabozorg[a], Ngoc Nguyen[b], Zhangxin Chen[b]

[a] Computer Modelling Group Ltd, Canada
[b] Department of Chemical and Petroleum Engineering, University of Calgary, Canada

ARTICLE INFO

Keywords:
Low salinity waterflooding
Chemical flooding
Hybrid EOR
Artificial intelligence
Probabilistic forecasting

ABSTRACT

Over the past decades, it has been widely shown that Low Salinity Waterflooding (LSW) outperformed High Salinity Waterflooding (HSW) in terms of higher oil recovery, particularly in combining with other conventional Enhanced Oil Recovery (EOR) methods such as chemical flooding to benefit from their synergies. This paper presents a novel approach to mechanistically model Hybrid Low Salinity Chemical Flooding, with: (1) development of a hybrid EOR concept from past decades; (2) utilizing a Multilayer Neural Network (ML-NN) artificial intelligent technique in a robust Equation-of-State reservoir simulator fully coupled with geochemistry; (3) systematic validation with laboratory data; and (4) uncertainty assessment of the LSW process at the field scale.

Various parameters such as polymer, surfactant, and salinity can affect on the relative permeability simultaneously during hybrid recovery processes. To overcome this problem, the ML-NN technique was applied for multidimensional interpolation of the relative permeability. Additionally, ML-NN was used within a Bayesian workflow to capture the uncertainties in both history matching and forecasting stages of LSW at field scale. The proposed model indicated good agreements with various coreflooding experiments including HSW, LSW, and Low Salinity Surfactant flooding (LSS), where it can efficiently capture the complex geochemistry, wettability alteration, microemulsion phase behavior, and the synergies occurring in these hybrid processes.

1. Introduction

Chemical flooding is important in EOR for improving recovery factor in mature reservoirs [5]. Alkaline has been used in the USA since 1929 to generate in-situ surfactant based on its reaction with acidic components in crude oil. Surfactant-based methods, for example, surfactant flooding, micellar-polymer flooding, and Alkaline-Surfactant-Polymer flooding (ASP), can effectively displace residual oil by decreasing oil-water interfacial tension (IFT) to ultra-low values. Polymer is often added into a chemical slug to improve sweep efficiency both vertically and aerially due to a higher viscosity of a polymer solution than that of water.

LSW is an emerging attractive EOR method and numerous studies in the past decades reported the benefits of LSW at the laboratory and field scales. Details on the development of the LSW process can be found in Dang et al. [6]. The recovery mechanisms of LSW are still open for discussion; however, wettability alteration in LSW has been observed in many coreflooding experiments. Up until now, wettability alteration is widely accepted as the primary mechanism for the incremental oil production by LSW. Past experimental studies have also indicated that LSW can alter the shape and endpoints of water and oil relative permeability [50,30,42,16,46]. Numerous laboratory measurements found that the effectiveness of LSW depends on composition of formation water, initial wettability condition, injected fluid composition, and reservoir rock [38,7,18,43].

Recently, hybrid EOR processes have been proposed in which LSW is combined with chemical flooding, e.g. LSS and Low Salinity Polymer flooding (LSP), to promote the synergies among these processes. Alagic and Skauge [1] reported that a coreflood experiment of combined LSW and surfactant flooding after secondary LSW help to achieve a relatively low residual oil saturation of about 6% with the final recovery factor of 92.3%. This study also indicated that significantly higher oil recovery about 10–13% Original Oil in Place (OOIP) was achieved when a surfactant solution was injected with low salinity brine compared to the one at high salinity. Johannessen and Spildo [22] performed different surfactant flooding with Berea sandstone at low salinity and optimal salinity. The obtained results revealed that LSS floods gave a moderate reduction in IFT (0.02 dynes/cm) with an ultimate recovery factor of up

* Corresponding author.
E-mail address: cuong.dang@cmgl.ca (C. Dang).

https://doi.org/10.1016/j.fuel.2019.116445
Received 19 July 2019; Received in revised form 27 September 2019; Accepted 16 October 2019
Available online 29 October 2019
0016-2361/

to 90% OOIP. The capillary number during surfactant flooding at optimal salinity was significantly higher than the one in LSS; but the final recovery factor and residual oil saturation were relatively similar to LSS. More importantly, all of the surfactant experiments at the optimal salinity exhibited higher surfactant retention than LSS. Average surfactant adsorption was about 0.39 mg/g rock for the optimal salinity surfactant flooding and 0.24 mg/g rock for LSS experiments. These results are similar to the ones obtained by Glover et al. [17] in which adsorption increases with increasing salinity. Tavassoli et al. [48] indicated that surfactant retention is high at salinities associated with Type II Winsor phase behavior where microemulsion is trapped in pores. However, it could be remobilized by LSW and the phase behavior reverses to Type I when the injected salinity is typically 70% of the optimal salinity. Johannessen and Spildo [23] compared performances of LSS (2500 ppm) and HSS (15,000–26,000 ppm) followed either by LSP or High Salinity Polymer flooding (HSP). Both LSS and HSS were conducted at the similar Winsor Type I phase behavior. Recovery factor after LSW was about 56% and the LSS followed by LSP increased the ultimate recovery factor up to 76%. On the other hand, the initial HSW provided a recovery factor of 51% and the final recovery after HSS and HSP was around 63% OOIP. In another study, Spildo et al. [47] attempted to minimize surfactant retention at relatively low IFT. It has been found that there were regions in the Winsor type I, where the IFT was low (0.01 – 0.1 dynes/cm) with good solubilization ratios. Additionally, surfactant retention in these regions was significantly lower than that at the Type III salinity. Based on these results, they suggested that LSS with Winsor type I could be a new strategy for low costs and effective surfactant injection. Teklu et al. [49] reported that LSS followed by CO_2 flooding could provide incremental oil recovery up to 25% beyond seawater flooding in a tight carbonate formation. Khanamiri et al. [25] observed that tertiary LSS after LSW showed good performance in different Berea corefloods. This enables the use of large variety surfactants with lower adsorption that are not applicable at higher salinities. Consequently, these advantages may result in more cost-effective and more environmentally friendly chemical EOR implementations.

Although LSS has been considered as a promising method for EOR, most studies published in the literature were based on coreflooding experiments. Several approaches were proposed to model chemical EOR processes [4,37,14,35,27,26,41,15] and LSW [21,13,6,9,2,28]; however, the capability of a reservoir simulator to mechanistically model a hybrid EOR process (e.g., LSS) is limited. After the benefits of hybrid low salinity chemical flooding were confirmed in the laboratory, a few preliminary numerical studies have been conducted to simulate 1D LSS coreflooding experiments. Skauge et al. [45] used an extended black oil model and a research chemical flooding simulator to capture the incremental oil recovery by LSW and LSS. Wettability alteration based on relative permeability modification was assumed as the sole mechanism for the underlying hybrid recovery process. In fact, as emphasized in one of the conclusions drawn from this study, the mechanisms behind LSS are far more complex than the pure wettability alteration. Tavassoli et al. [48] presented an approach for modeling LSS by coupling UTCHEM and IPHREEQC software. UTCHEM – a research chemical flooding simulator developed at the University of Texas was used to simulate surfactant flooding, whereas IPHREEQC – a geochemical package developed by U.S. Geological Survey was used for modeling reactive flow. The mass conservative equations were solved in UTCHEM transferred to IPHREEQC to calculate a new equilibrium state. It was recognized from the previous studies that the UTCHEM and IPHREEQC's coupling can be computationally expensive [35]. More importantly, the simultaneous effects of salinity and surfactant on relative permeability modeling were not addressed in this work. Dang et al. [10,11] simulated the benefits of a hybrid ASP flooding process by combining secondary low salinity waterflooding with tertiary ASP flooding using an Equation-of-State reservoir simulator and the results indicated that hybrid ASP flooding provided 10% incremental oil recovery over the conventional high salinity ASP flooding. However, LSW and chemical flooding slugs were injected sequentially, and, therefore, the interactions among low salinity brine, surfactant solution, and reservoir rock were neglected.

To adequately quantify the effectiveness of hybrid low salinity chemical flooding in both laboratory and field scales, it is important to develop a comprehensive model that can capture different recovery mechanisms from macroscopic to microscopic scales for the underlying process. The modeling approach must also be able to capture complex phenomena occurring in a hybrid recovery method, e.g., various parameters (salinity, surfactant and polymer) that can simultaneously affect relative permeability curves during a course of low salinity chemical flooding. The new development of artificial intelligence can play an important role to overcome these issues [3,31–33]. This paper presents a new approach for mechanistically modeling hybrid EOR processes using artificial intelligence based on the Multilayer Neural Network (ML-NN) technique. This helps to capture important physics and address the multi-dimensional challenge of relative permeability interpolation.

2. Modeling hybrid LSS flooding

The combination of LSW and surfactant flooding, called Hybrid low salinity surfactant flooding, is a multi-mechanistic process because it incorporates different recovery mechanisms in a single recovery method, such as wettability alteration of LSW, a IFT reduction of surfactant flooding, and improved sweep efficiency of polymer flooding.

To model complex hybrid EOR processes, it is important to take into account important physics that occur in chemical EOR and LSW as well as the complicated interactions among different chemicals, brine, rock, and crude oil (Fig. 1). Nghiem et al.'s model [40] was applied to simulate complex geochemical reactions occurred in hybrid low salinity surfactant recovery process. LSW modeling was extended from Dang et al.'s models [6,9], and coupled with Nghiem et al.'s model [39] to capture microemulsion phase behavior and polymer rheology properties in the chemical EOR. More importantly, the ML-NN algorithm was applied to the relative permeability interpolation under the simultaneous effects of salinity and surfactant in the LSS process. The proposed modeling workflow was implemented in an Equation-of-State (EOS) compositional reservoir simulator. The important features of LSS modeling approach are highlighted below.

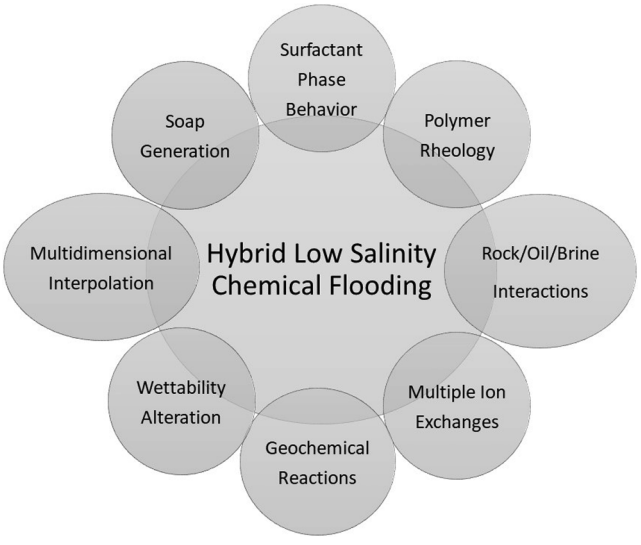

Fig. 1. Important physics in hybrid low salinity chemical flooding.

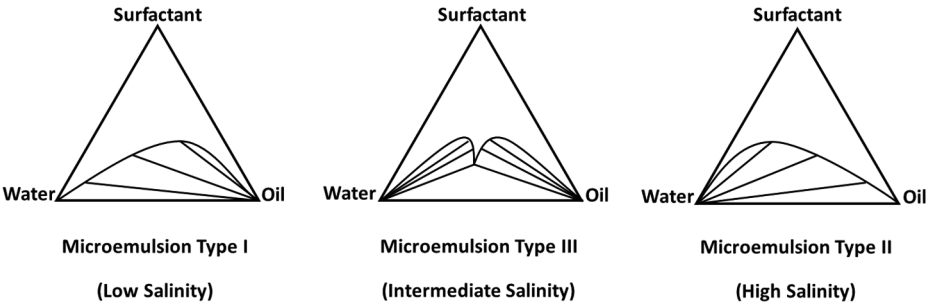

Fig. 2. Microemulsion phase behavior as a function of salinity.

2.1. Microemulsion phase behavior modeling

It was recognized that microemulsion phase behavior in surfactant-based methods strongly depends on salinity (Fig. 2). At type III phase behavior, the system can have up to three phases: water, oil, and microemulsion [19]. Several proposed ASP models in the literature required the modeling of Type III microemulsion [37,28,48]; however, Sheng [44] indicated that field-scale ASP simulation needs a simplified model to reduce the complexity of the modeling process. To overcome this challenge, Nghiem et al. [39] implemented an alternative solution that allows modeling a surfactant-based recovery method without the need of introducing the third microemulsion phase. Nghiem's modeling used an approximating Type III with two pseudo phases oil and water based on the solubility data as introduced by Jong et al. [24] shown in Fig. 3. This approach has been applied to successfully history match numerous ASP coreflood experiments with different chemical formulations, core properties, and injection schemes [10,11].

Huh [20] indicated that microemulsion/oil and microemulsion/water IFT in surfactant-based recovery methods can be calculated from solubilization ratios (Fig. 4). This approach was also applied to calculate IFT in pseudo oil-water system used in this study.

2.2. Geochemistry modeling

Geochemistry plays a critical role in LSW and chemical EOR processes. However, reservoir simulators and specialized chemical flooding software often need to be coupled with another geochemistry module, e.g., EQBATCH (Bhuyan, 1989; [37], PHREEQC or IPHREEQC [51,52,14,28] for geochemical modeling. The external coupling to these geochemistry modules could be time consuming equations [12,35] that prevents the application at large scales. This study used an efficient approach for fully-coupled geochemical compositional reservoir simulation to model important reactions in the chemical EOR and LSW processes as shown below.

Chemical equilibrium reactions, i.e.:

$$H^+ + OH^- \leftrightarrow H_2O \quad (1)$$

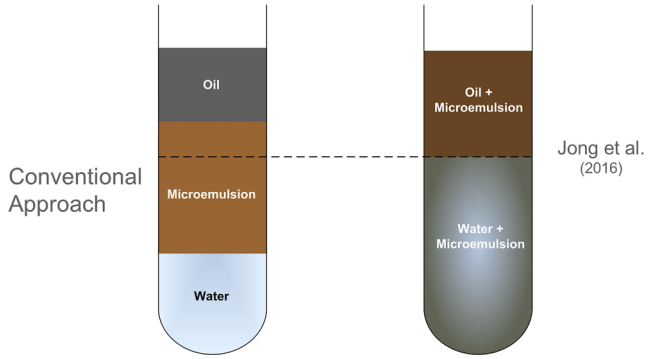

Fig. 3. Modeling of microemulsion phase behavior.

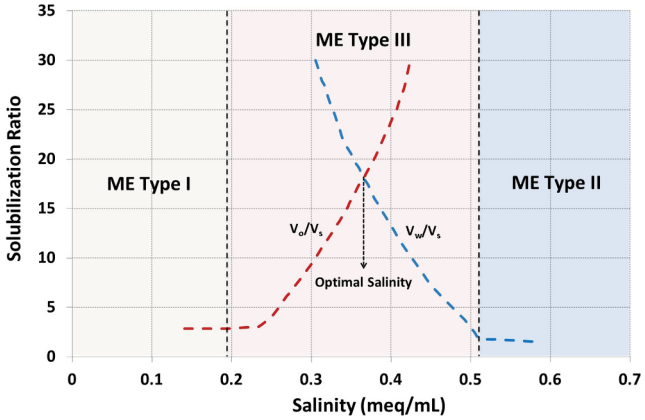

Fig. 4. Solubilization ratios in ASP flooding.

$$H^+ + CO_3^{--} \leftrightarrow HCO_3^- \quad (2)$$

$$H^+ + NaCO_3^- \leftrightarrow Na^+ + HCO_3^- \quad (3)$$

$$NaHCO_3 \leftrightarrow Na^+ + HCO_3^- \quad (4)$$

$$H^+ + NaOH \rightarrow Na^+ + H_2O \quad (5)$$

Rate dependent reactions, i.e.

$$H^+ + Calcite \rightarrow Ca^{++} + HCO_3^- \quad (6)$$

$$H^+ + Magnesite \rightarrow Mg^{++} + HCO_3^- \quad (7)$$

$$4OH^- + 3H_2O + Kaolinite \rightarrow 2Al(OH)_4^- + 2H_3SiO_4^- \quad (8)$$

Multiple ion exchange

$$H - X + Na^+ \leftrightarrow Na - X + H^+ \quad (9)$$

$$Na^+ + \frac{1}{2}(Ca - X_2) \leftrightarrow (Na - X) + \frac{1}{2}Ca^{++} \quad (10)$$

$$Na^+ + \frac{1}{2}(Mg - X_2) \leftrightarrow (Mg - X) + \frac{1}{2}Ca^{++} \quad (11)$$

2.3. Polymer rheology modeling

Polymer rheology is important in polymer-based EOR methods. The model used in this paper takes into account the following phenomena:

- Salinity dependent polymer viscosity
- Shear rate dependent polymer viscosity
- Polymer retention
- Permeability reduction
- Polymer degradation

2.4. Wettability alteration modeling

Generally, LSW process can alter the initial reservoir wettability condition, e.g. from oil wetness to water wetness, and this phenomenon can be modeled by considering multiple relative permeability sets that represent HSW and LSW [9,29]. Several interpolation parameters, e.g., salinity, ion exchange, surface complexation, and mineral dissolution, have been proposed in the literature. In this study, multiple-ion exchanges based interpolation [9] was used to interpolate between different wettability alteration conditions.

2.5. Multi-layer neural network algorithm for relative permeability interpolation

As observed from laboratory experiments, several factors, e.g., salinity, surfactant, and polymer with a viscoelastic effect, can change the shape and endpoints of relative permeability curves simultaneously. This problem has been found in many advanced EOR methods, e.g. chemical assisted gas flooding, low salinity WAG, or CoSolvent-Steam injection; however, it has been rarely discussed in the past. To overcome this problem, an ML-NN technique [3] was utilized for multi-dimensional interpolation of oil and water relative permeabilities in LSS process.

The basic architecture of ML-NN consists of multiple layers (Input, Hidden, and Output) as shown in Fig. 5. Based on the original training data, all weight matrices of the *N* hidden layers and the weight factor of the output layer are calculated. Consequently, the mean-square error for a given weight distribution is minimized below:

$$E^2(\vec{w}) = \frac{1}{N-1}\sum_{i=1}^{N}[\theta(\vec{x}^{(i)}) - \tilde{\theta}(\vec{x}^{(i)}, \vec{w})]^2 \tag{12}$$

where θ and $\tilde{\theta}$ are the outputs for the objective function from a simulator and a proxy model, respectively. In hybrid low salinity chemical flooding modeling, θ stands for relative permeability, vector $\vec{x}$ defines the input values of saturation, salinity and IFT, and vector $\vec{w}$ represents the network weights. The gradient error information is propagated back every time for the set of prediction as shown in Fig. 6.

One hidden layer containing three neurons was used for LSW's relative permeability interpolation because the limited amount of training data makes a deeper network an overfitting tool. A simple sigmoid:

$$S(x) = \frac{1}{1+e^{-x}} \tag{13}$$

is used as an activation function, as the output value of relative permeability is naturally positive and normalized to 1.

Numerous gradient-based algorithms of ML NN optimization have been introduced in the literature and different versions of the Stochastic Gradient Descent (SGD) method have recently gained a lot of popularity in the context of Deep Learning Network training. However, for this simple network model it has been found that the Levenberg-Marquardt algorithm provided noticeably faster training convergence and a smaller mean square error for training data. This algorithm, therefore, is used as an ML-NN optimization. It updates the ML NN weights to find such a weight correction $\vec{h}$ that minimizes $E^2(\vec{w}+\vec{h})$ where $\vec{w}$ stands for the current weight. It can be shown that such minimization naturally occurs if at each iteration the correction $\vec{h}$ satisfies the following equation:

$$[\hat{J}^T\hat{J} + \mu\hat{I}]\vec{h} = \hat{J}^T[\tilde{\vec{\theta}} - \vec{\theta}] \tag{14}$$

where $\hat{J}$ is a Jacobian, $\hat{I}$ is an identity matrix, and μ is a control parameter balancing between Gradient ($\mu \to \infty$) and Newtonian ($\mu \to 0$) algorithms. The derivatives of an objective function with respect to the NN weights are calculated analytically by applying a chain rule.

The training data consists of different sets of relative permeability curves experimentally measured at different combinations of saturation, salinity and IFT. In this case, two criteria for the method efficiency were defined: (1) fast convergence to a very small value of a mean-square error for the training data, and (2) good matching with actual coreflooding measurements.

Fig. 7 shows the workflow of ML-NN implementation that utilizes Levenberg-Marquardt algorithm of the Neural Network optimization.

Fig. 8 shows the results for 2D relative permeability interpolation of a pure LSW process using ML-NN with the NN configuration of 1 hidden layer containing 3 neurons. The interpolation was based on the training k_{ro} and k_{rw} curves for HSW and LSW taken from Dang et al. [8].

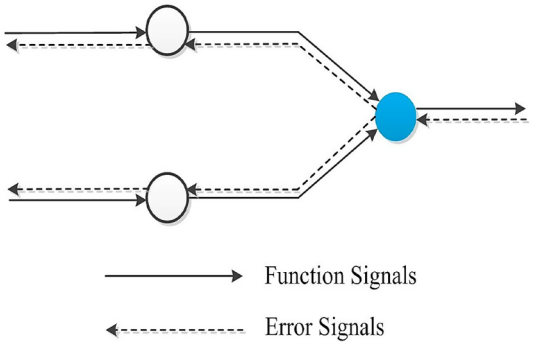

Fig. 6. Flow of the feedforward prediction and backward error in ML-NN training.

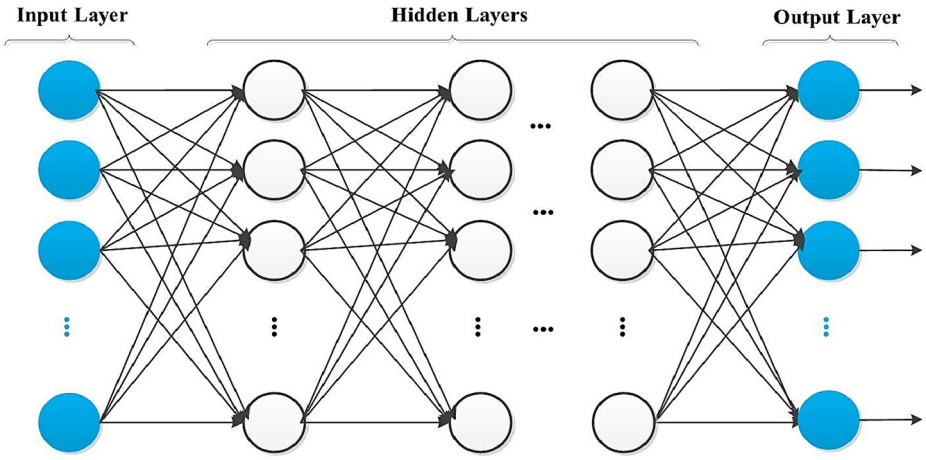

Fig. 5. Basic multi-layer neural network architecture.

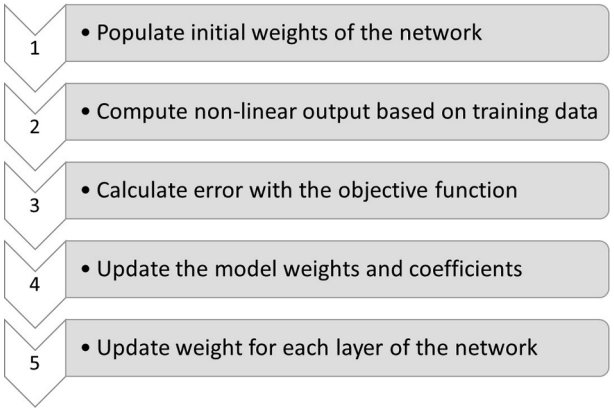

Fig. 7. ML-NN algorithm.

In contrast with pure LSW, the LSS process requires higher dimensional interpolation for relative permeability curves because both salinity and surfactant can alter the shape and endpoints of the relative permeability. Figs. 9 and 10 show ML-NN prediction for 3D interpolation of the LSS process using two hidden layers containing (4, 4) neurons. The experimental data for relative permeability for NN training was taken from Alagic and Skauge [1] and Tavassoli et al. [48]. 3D interpolation for relative permeability was applied in LSS coreflood simulation in the next section.

3. Model validations

The proposed model equipped with the ML-NN algorithm was validated against different laboratory corefloods performed by Alagic and Skauge [1] for: (1) seawater flooding (HSW); (2) LSW; and (3) tertiary LSS.

3.1. Coreflooding description and 1D simulation model

Alagic and Skauge [1] conducted several experiments to evaluate performances of LSW and LSS processes in comparison with secondary seawater flooding and tertiary LSS after seawater flooding. Fig. 11 shows the experimental setup and injection schemes for two corefloods (B1 and B3) used in this paper. Core properties and injection composition are shown in Tables 1 and 2. Seawater was used as the connate brine for all experiments with total dissolved solids of 36,321 ppm. Then, seawater and low salinity brine containing 0.5 wt% NaCl were injected at S_{oi} in the first step for cores B3 and B1, respectively. In the second step, LSS was applied to investigate the potential of this hybrid process on reducing residual saturation. Pressure changes and effluent compositions were monitored and the injection rate was about 0.1cm^3/min for all the experiments.

The simulation was performed with a 1D vertical model that consisted of 50 grid blocks. Important physics presented in the previous section have been included in the model, e.g., microemulsion phase behavior, chemical equilibrium reactions, rate dependent reactions, multiple ion-exchange, wettability alteration, and IFT reduction. The relative permeability endpoints were measured in the laboratory by Alagic and Skauge [1] and reproduced by Tavassoli et al. [48] as shown in Fig. 12. A solubilization ratio for surfactant phase behavior modeling

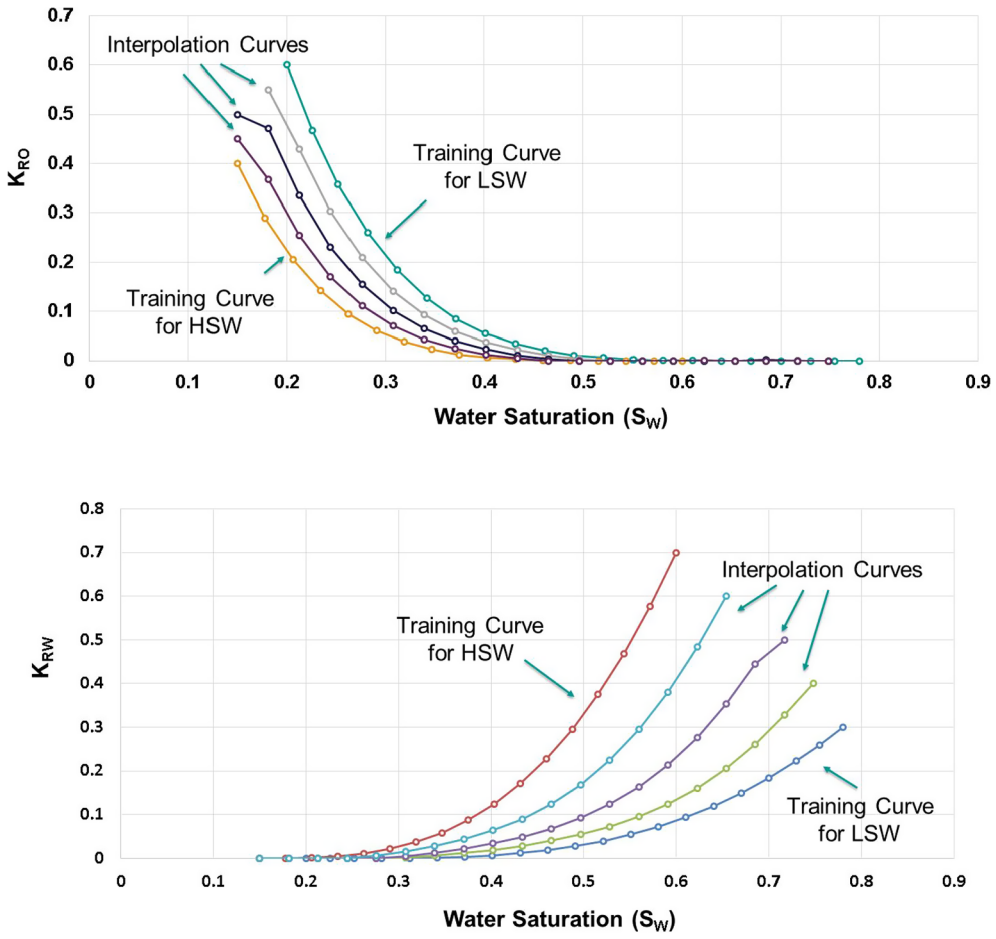

Fig. 8. Application of ML-NN for relative permeability interpolation in LSW process.

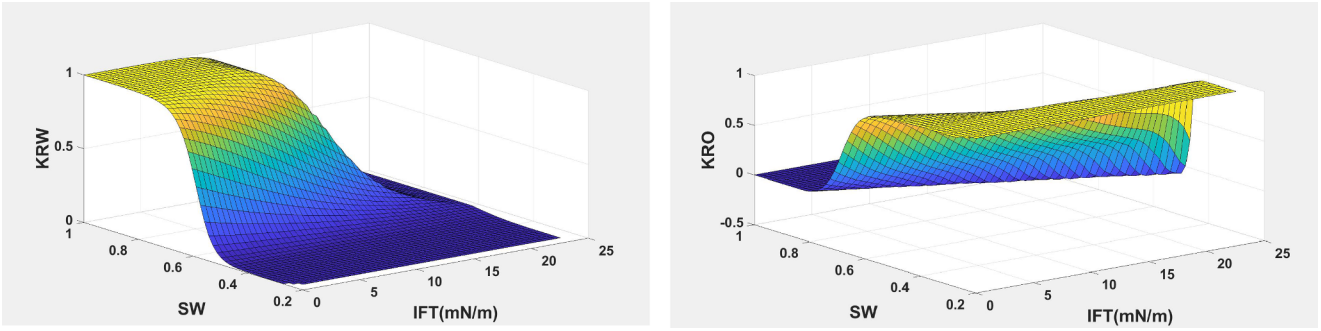

Fig. 9. 3D interpolation of K_{ro} and K_{rw} for LSS using ML-NN (Salinity = 15,440 ppm).

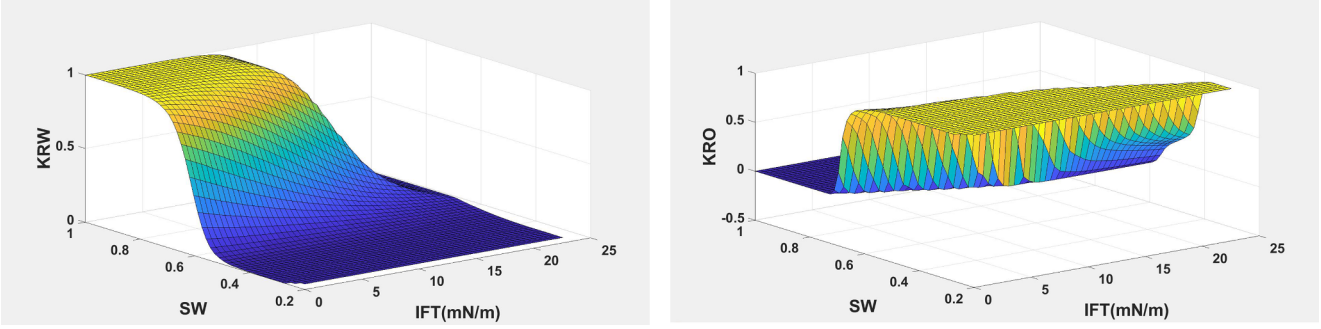

Fig. 10. 3D interpolation of K_{ro} and K_{rw} for LSS using ML-NN (Salinity = 25,880 ppm).

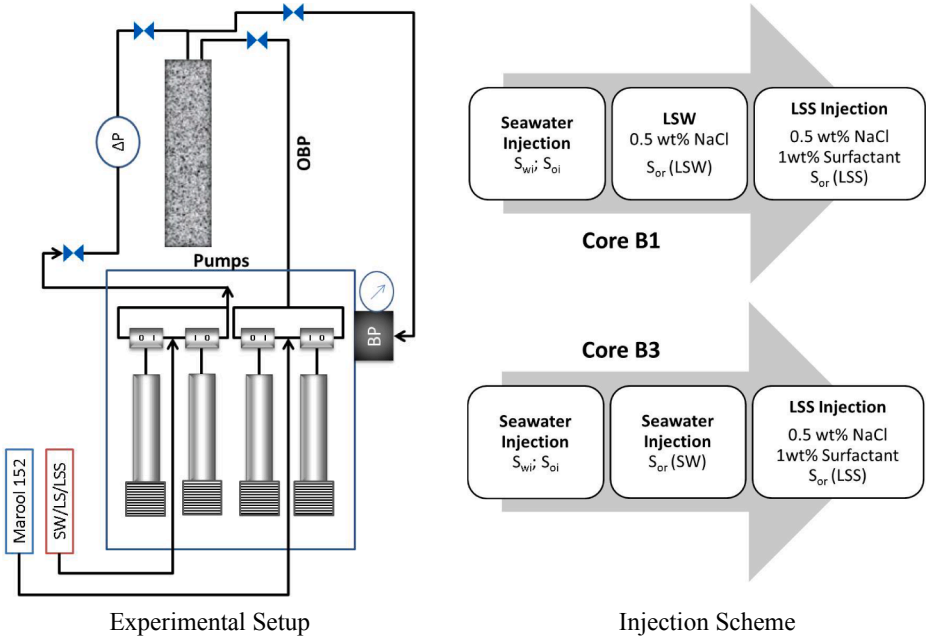

Fig. 11. Alagic and Skauge's [1] coreflood description.

Table 1
Core properties for Alagic and Skauge's [1] experiment.

Core ID	B1	B3
Rock type	Berea sandstone	Berea sandstone
Length (cm)	7.92	8.1
Diameter (cm)	3.7	3.73
S_{wi}	0.24	0.24
S_{oi}	0.76	0.76
Porosity (%)	22.6	23.1
Permeability (mD)	630	715

Table 2
Brine composition of SW and LSW [1].

Composition	SW	LSW
Ca^{++}(ppm)	471	0
Na^{+}(ppm)	11,159	1960
Mg^{++}(ppm)	1329	0
Cl^{-}(ppm)	20,130	3040
SO_4^{-}(ppm)	2740	0
HCO_3^{-}(ppm)	142	0
K^{+}(ppm)	349	0

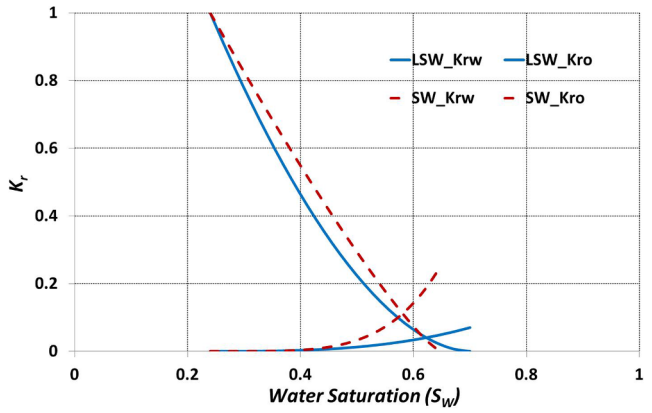

Fig. 12. Relative permeability curves for SW and LSW floods [48]

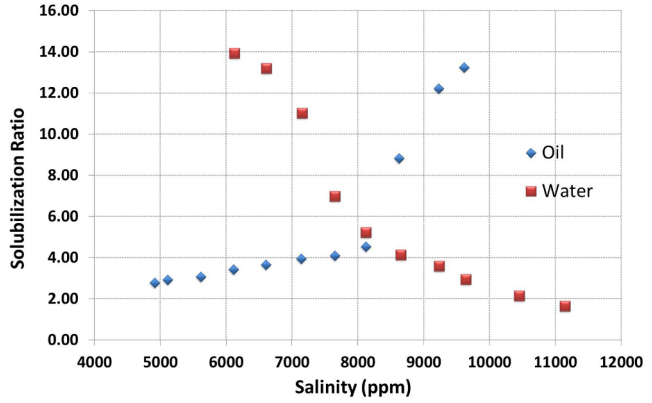

Fig. 13. Laboratory solubilization ratios for LSS [48]

(Fig. 13) was taken from Tavassoli et al. [48].

3.2. Simulation of high salinity waterflooding

The proposed model has been applied to match a production profile of seawater injection in core B3 as reported by Alagic and Skauge [1]. The composition of injected seawater was similar to the one in formation water. Therefore, wettability alteration was not included in the model. The oil recovery factor after a continuous injection of 7 pore volumes of seawater was about 54.6%. The proposed model provided a very good match with the coreflooding data in terms of the final oil recovery factor and the breakthrough time of oil production by seawater injection as shown in Fig. 14.

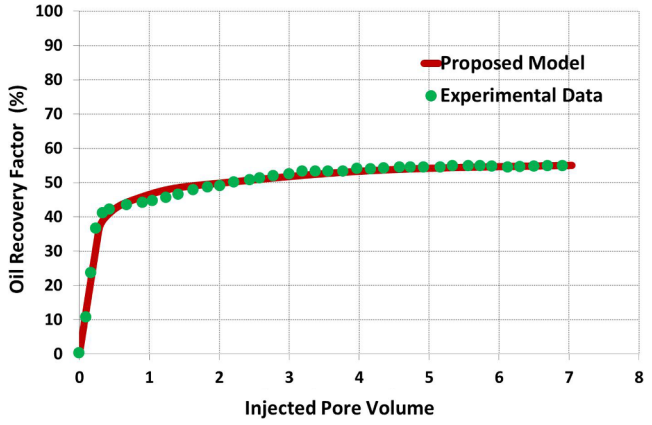

Fig. 14. Oil recovery factor for HSW.

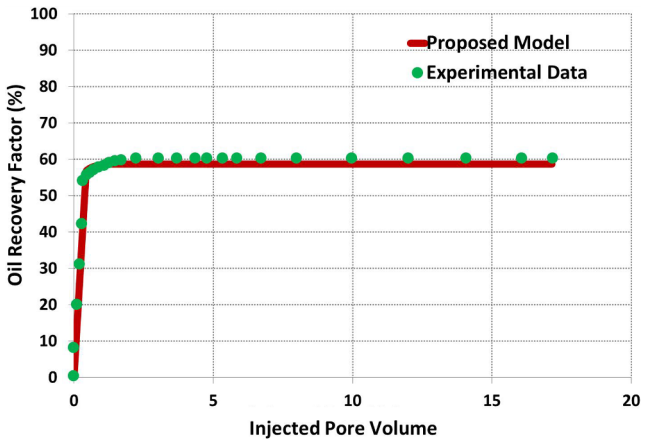

Fig. 15. Oil recovery factor for LSW.

3.3. Simulation of low salinity Waterflooding

Coreflooding B1 was similar to B3 except that a continuous low salinity brine of 0.5 wt% NaCl was injected for about 17 pore volumes. Fig. 15 shows the cumulative recovery factor by LSW from the proposed model along with the experimental data. There was a good agreement between simulation and laboratory measurements of the LSW process in which the ultimate recovery factor was about 60.2%. In comparison with HSW in the B3 coreflood experiment, incremental oil recovery was about 5.6% by LSW due to a favorable wettability alteration toward more water wetness. Fig. 16 shows the pressure drop calculated from the proposed model against the one monitored during the experiment. In consistent with the laboratory data, the simulation results indicated that additional oil was produced during the first 2 to 3 PV with slight changes in the pressure drop profile. Small traces of fines accumulation were detected by Alagic and Skauge [1] that may explain for a partial increase in the pressure drop profile observed at the end of the LSW process.

Figs. 17 through 19 show the comparison between simulation and laboratory data for the ion concentration at the effluent during LSW for Na^+, Ca^{++}, and Mg^{++}, respectively. As shown in these figures, the ionic composition of the produced water gradually decreases during the first periods of LSW. This matching result is achieved by considering multiple ion-exchanges between injected brine and reservoir rock, and geochemical reactions occurred during the course of LSW process.

3.4. Simulation of low salinity surfactant flooding

After the first step of LSW, Alagic and Skauge [1] extended the B1

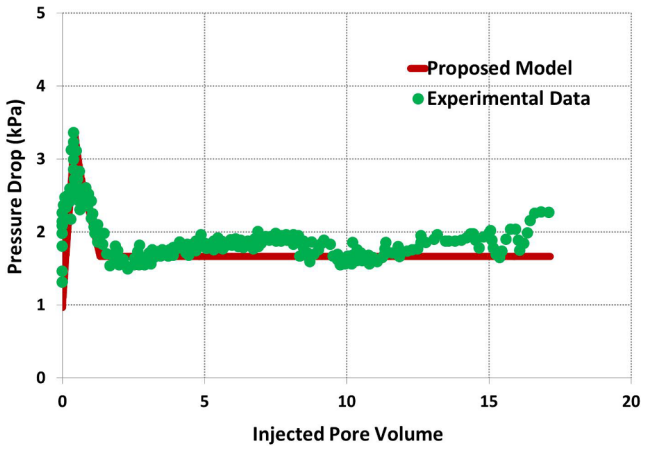

Fig. 16. Pressure drop for LSW.

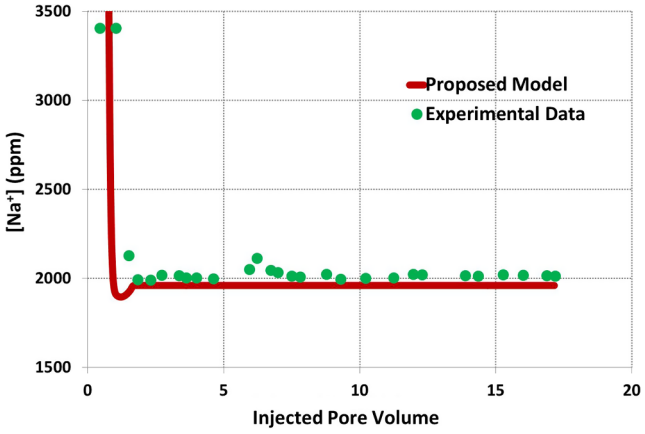

Fig. 17. Na^+ effluent for LSW.

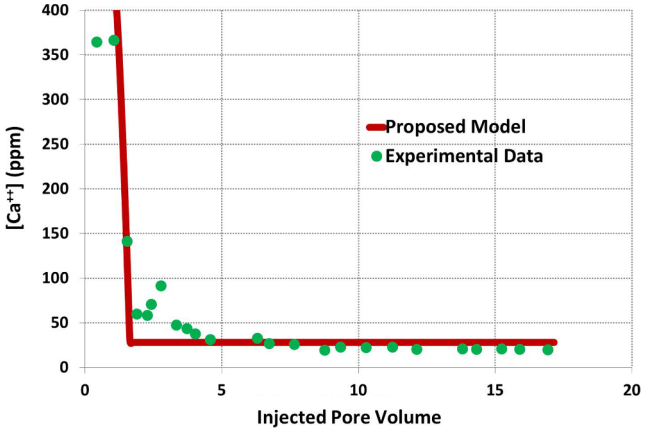

Fig. 18. Ca^{++} effluent for LSW.

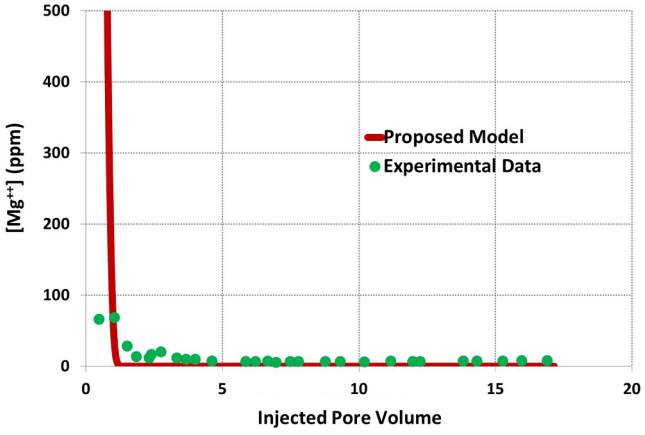

Fig. 19. Mg^{++} effluent for LSW.

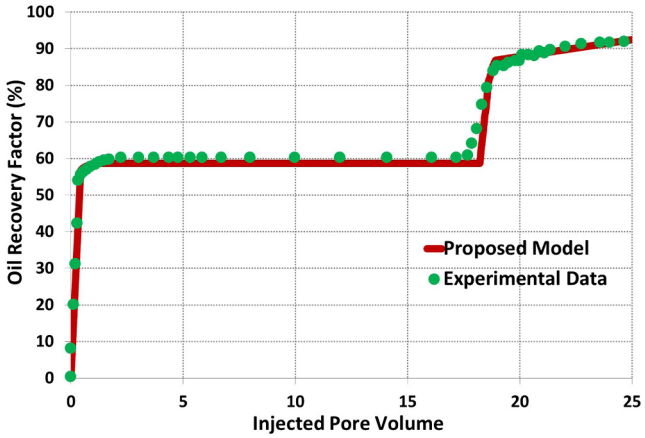

Fig. 20. Oil recovery factor for LSS Flooding.

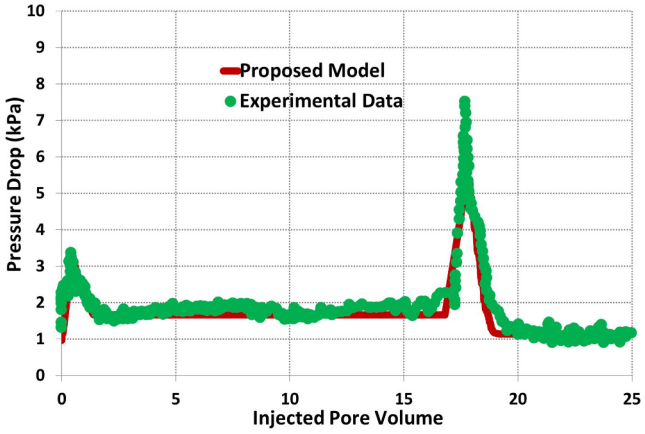

Fig. 21. Pressure drop for LSS Flooding.

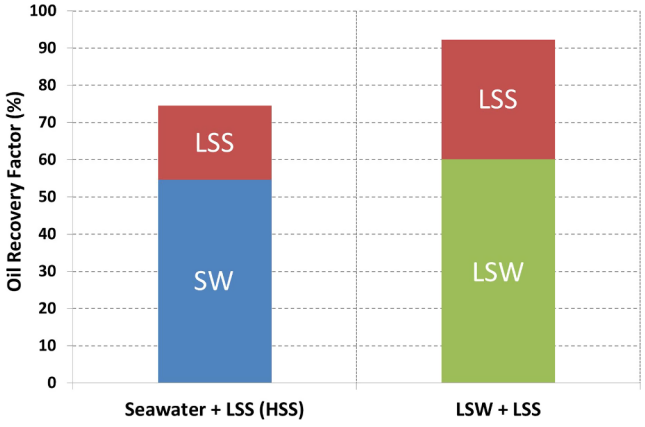

Fig. 22. Comparison between HSS Flooding and LSS Flooding.

experiment by injecting a continuous low salinity surfactant solution. The surfactant slug consisted of 0.5 wt% NaCl, 1 wt% Enordet surfactant, and 1 wt% isoamyl alcohol with the solubilization ratios indicated in Fig. 13. The new mechanistic model equipped the with ML-NN artificial intelligence algorithm has been used to perform 3D interpolation of relative permeability under the simultaneous effects of salinity and surfactant. The architecture of Levenberg-Marquardt neural network used in this case study was one hidden layer containing 4 neurons. The neural network system is trained by laboratory data and provides a set of relative permeability curves for each grid block corresponding to its calculated values of IFT and salinity.

As experimentally found in the past studies, LSS flooding successfully reduced residual oil saturation after LSW with very low surfactant retention even though IFT was not ultra-low. Fig. 20 indicates that the proposed model with ML-NN efficiently captures the advantages of LSS with the final oil recovery factor over 90% OOIP. The calculated pressure drop from simulation results is also consistent with the one obtained from the laboratory experiment as shown in Fig. 21.

LSW followed by LSS demonstrated a superior performance over the conventional method when surfactant flooding is injected in a high salinity environment as shown in Fig. 22. The final recovery factory by continuous injection of LSS after seawater injection was about 74.5%

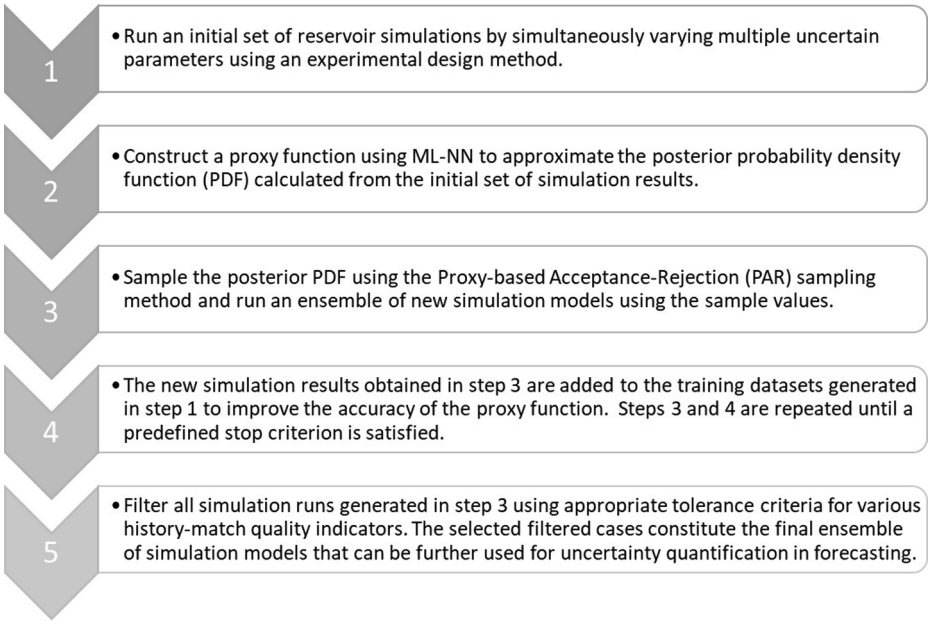

Fig. 23. Bayesian workflow using ML-NN.

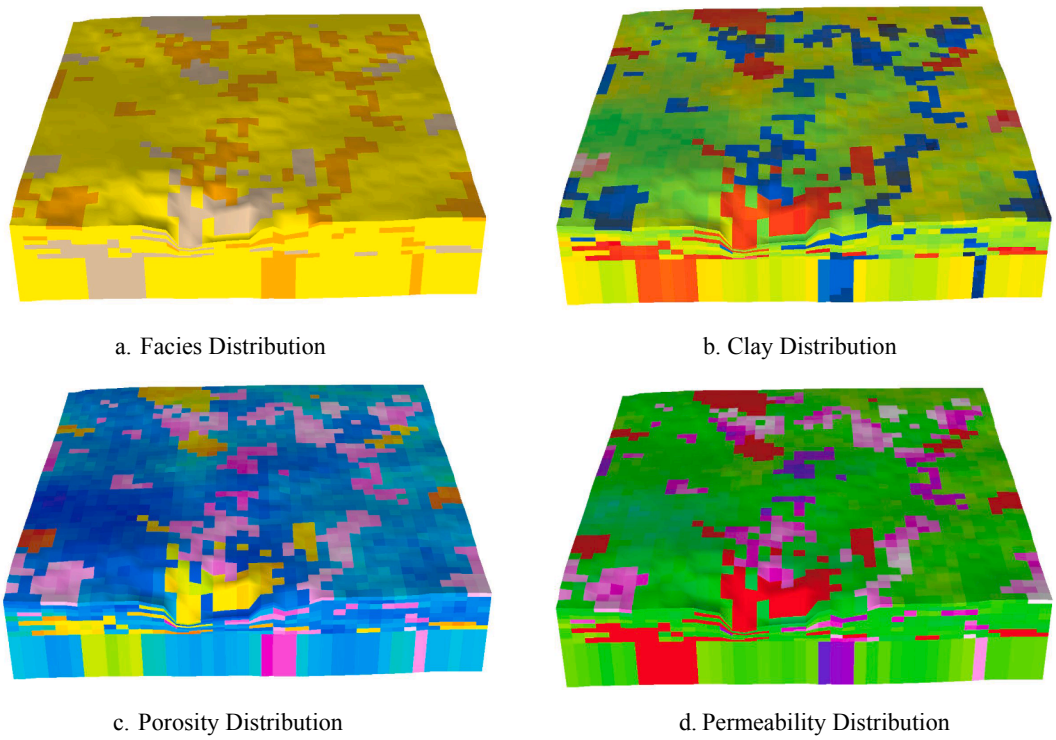

Fig. 24. Base Case for LSW History Matching.

compared to 92% by hybrid low salinity surfactant flooding. With a higher tertiary recovery factor and lower surfactant adsorption confirmed by different coreflood experiments, LSS can become an attractive and cost-effective method for the future EOR.

4. Application of ML-NN in quantifying uncertainties of LSW

Chemical EOR, LSW, and hybrid low salinity chemical flooding have been identified as strongly geology-dependent recovery processes. Uncertainties in these processes are associated with geology and relative permeability estimation due to the wettability alteration [7]. Thus, it is important to capture the uncertainties of geology and reservoir parameters in history matching (HM) and production forecasting of these processes. Yang et al. [53] introduced a Bayesian framework that can effectively evaluate the uncertainties in forecasting results. This approach has been extended in this study to quantify the uncertainties of the field-scale HM of the LSW process by utilizing ML-NN as a proxy. A detailed Bayesian workflow using ML-NN is described in Fig. 23. This approach was also compared with the classical algorithms such as Particle Swarm Optimization (PSO) [34] and Differential Evolution (DE) [36].

Field-scale LSW HM has been recognized as a complex task due to a

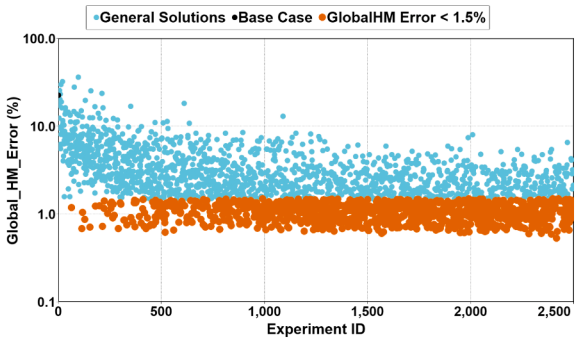

Particle Swarm Optimization

(Best Matched Model: Global Error = 0.53 %)

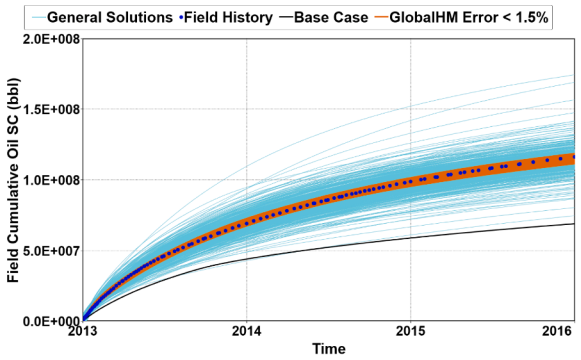

Particle Swarm Optimization

(Oil Production History Matching)

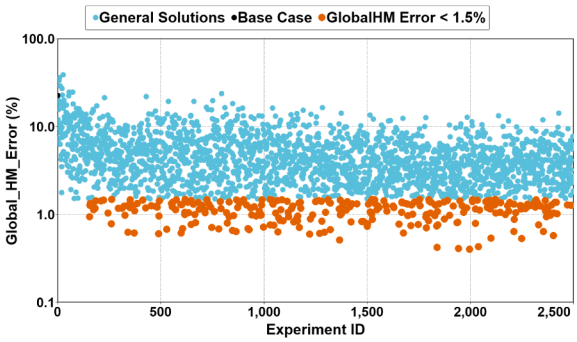

Differential Evolution

(Best Matched Model: Global Error = 0.4%)

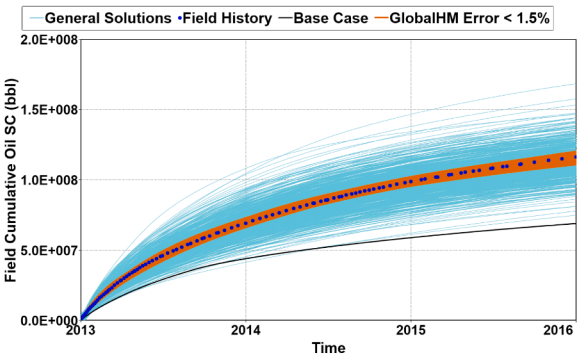

Differential Evolution

(Oil Production History Matching)

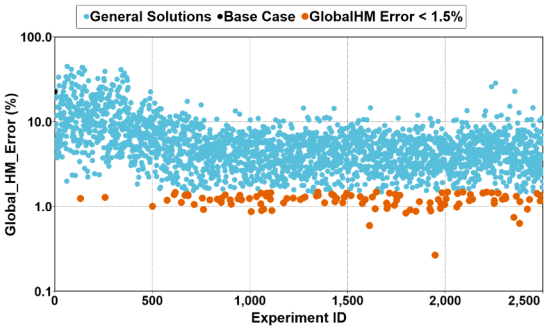

Bayesian Plus ML-NN

(Best Matched Model: Global Error = 0.26%)

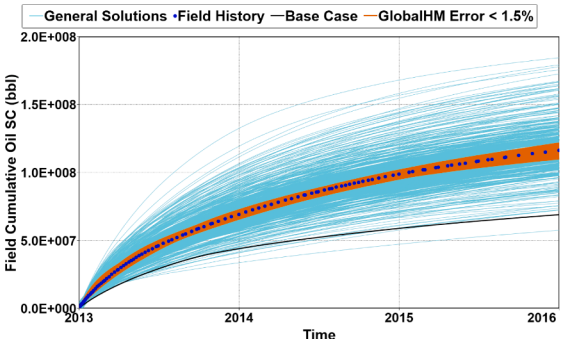

Bayesian Plus ML-NN

(Oil Production History Matching)

Fig. 25. Field-scale LSW history matching results.

large number of involved parameters. It is essential to simultaneously match both geological distribution and reservoir engineering parameters for achieving good history matching results. From this perspective, we used an integrated HM approach for LSW in which geological information is transferred to a simulation model smartly controlled by an optimizer in an automatic loop to provide the best global HM results. In this study, a Bayesian framework coupled with ML-NN algorithm, DE, and PSO were used for a LSW HM case described by Dang et al. [10,11]. The sandstone reservoir consists of 14,400 grid blocks with 3 different facies as shown in Fig. 24. LSW was applied in an inverted five-spot pattern. Multiple ion-exchange reactions between calcium, magnesium and clay surfaces are considered. The facies proportion and distribution in each layer and relative permeability parameters were adjusted to get the match with the production data.

Fig. 25 shows the comparison of HM results for this particular case study with 2500 simulation jobs for Bayesian plus ML-NN, DE, and PSO. All three algorithms can provide good HM results from a global history matching point of view; however, the best-matched model with the lowest global history matching error was found by the Bayesian method with ML-NN. More importantly, this approach demonstrates a better capability in quantifying the uncertainties of the LSW HM process since it provides better uncertainty ranges for all HM parameters, as indicated in Fig. 26 for Corey's relative permeability exponents and proportion of medium-sand facies in layer 1, compared to DE and PSO. This advantage is very important to take into account the uncertainties of LSW and hybrid low salinity chemical flooding in short and long term production forecasting (Fig. 27).

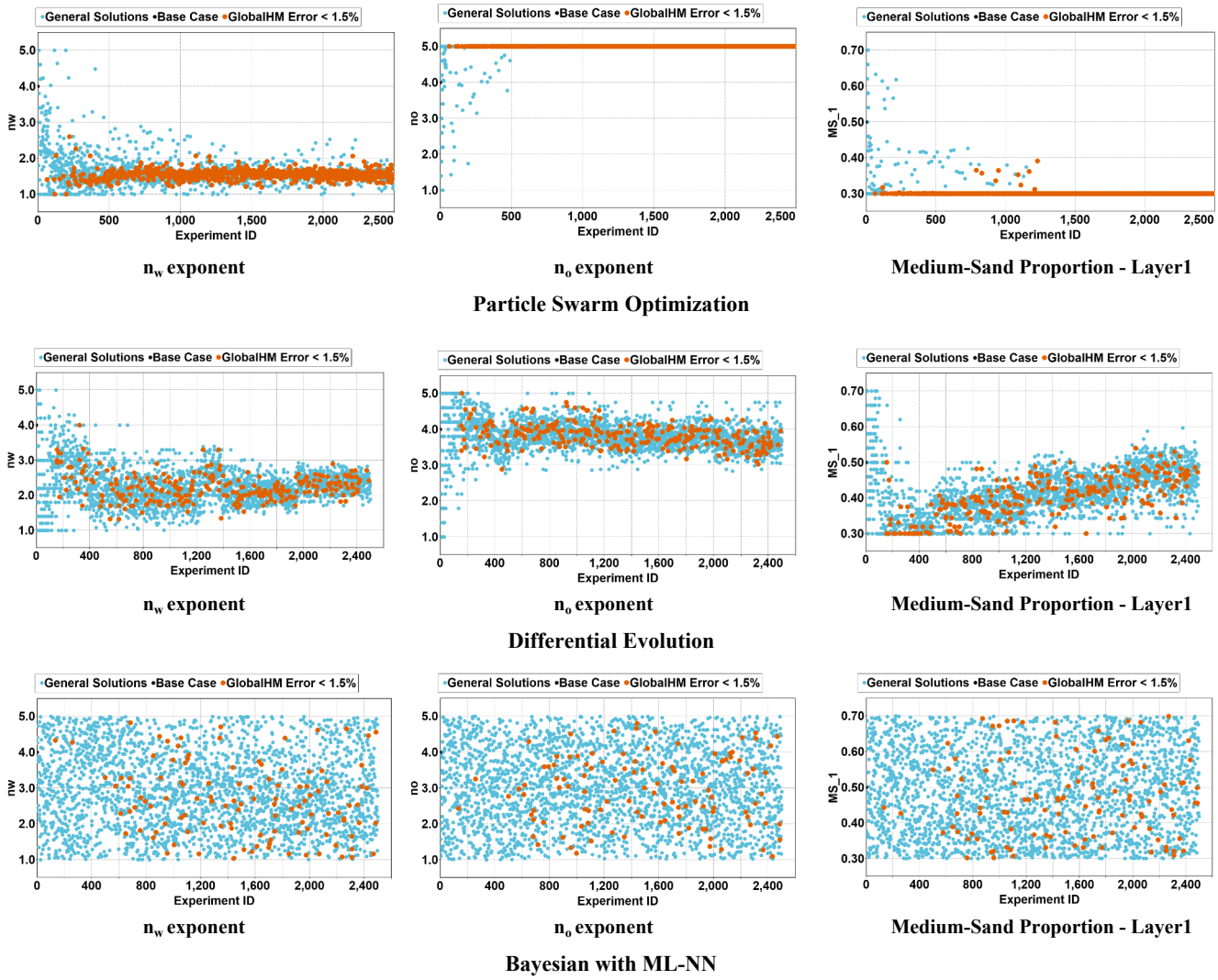

Fig. 26. Uncertainty assessment of LSW history match.

5. Further discussions for new applications

Relative permeability is important in predicting flow behaviors in porous media and adequately modeling displacement processes, especially for hybrid EOR methods that require multidimensional interpolation of the relative permeability. The application of artificial intelligence for estimating relative permeability proposed in this study can be efficiently applied to model different advanced recovery processes, for example:

- Hybrid Low Salinity Polymer Flooding when viscoelastic polymer and salinity can affect the relative permeability simultaneously.
- Hybrid Low Salinity Surfactant Polymer Flooding when surfactant, viscoelastic polymer and salinity can affect the relative permeability simultaneously.
- Hybrid Low Salinity WAG when CO_2 and salinity can affect the relative permeability simultaneously.
- Solvent assisted steam flooding in which solvent and steam can affect the relative permeability simultaneously.

Additionally, artificial intelligence (ML-NN algorithm) can be effectively applied to optimize complex EOR processes besides assisted history matching and uncertainty quantification of the hybrid low salinity chemical flooding process.

6. Conclusions

- A mechanistic model for hybrid low salinity chemical flooding is presented and implemented in an EOS compositional reservoir simulator.
- Artificial intelligence based ML-NN is used for multi-dimensional interpolation of the relative permeability in EOR processes.
- Hybrid LSS flooding is a promising EOR method as it provides a high recovery factor, up to 92% OOIP and low surfactant retention in laboratory tests.
- Simulation results based on the proposed model are strongly consistent with various coreflood data.
- A Bayesian workflow plus multi-layer neural network is an efficient and practical approach for LSW history matching and uncertainty assessment at the field scale.

Acknowledgements

The authors would like to acknowledge Dr. Vijay Shrivastava at Computer Modelling Group Ltd. for many fruitful technical discussions. The authors also thank Emerson-Paradigm for providing the GoCad™ software for this research. The compositional simulator GEM™ and the optimization software CMOST™ from Computer Modelling Group Ltd. were used in this paper. Part of the research is supported by NSERC/Energi Simulation and Alberta Innovates Chairs.

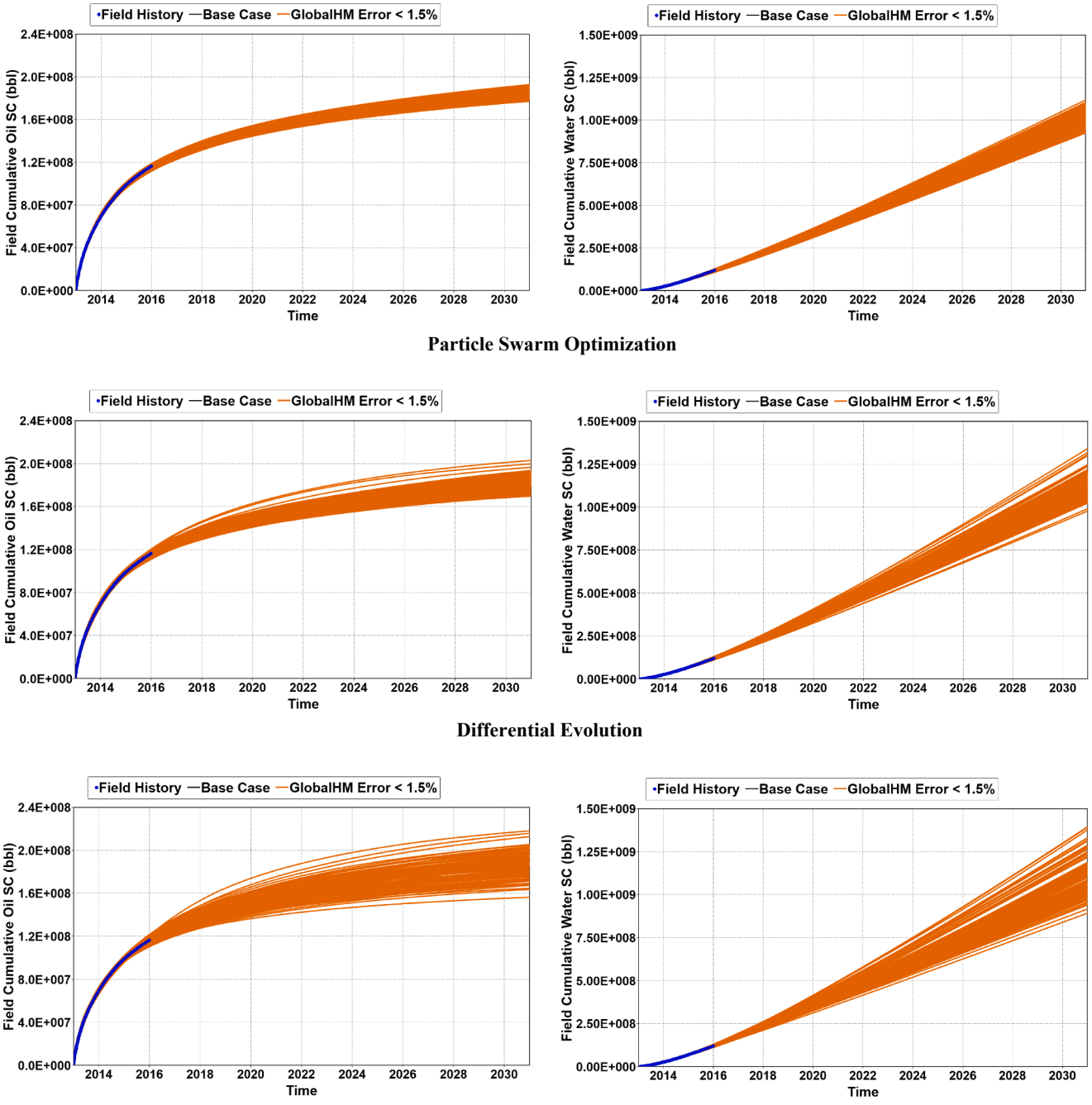

Fig. 27. Uncertainty quantification of LSW production forecasting.

References

[1] Alagic E, Skauge A. Combined low salinity brine injection and surfactant flooding in mixed-wet sandstone cores. Energy Fuels 2010;2010(24):3551–9.

[2] Al-Shalabi E. Modeling the Effect of Injecting Low Salinity Water on Oil Recovery from Carbonate Reservoirs (PhD Dissertation) Texas, USA: The University of Texas at Austin; 2014.

[3] Amirian E, Fedutenko E, Yang C, Chen Z, Nghiem L. Application of Data Management and Analysis. Springer 2018;P.1:2018.

[4] Chen Z, Ewing RE, Lazarov RD, Maliasso VS, Kuznetsov YA. Multilevel preconditioners for mixed methods for second order elliptic problems. Numer Lin Algebra Appl 1996;3(5):427–53.

[5] Chen Z, Huan G, Ma Y. Computational Methods for Multiphase Flows in Porous Media. Computational Science and Engineering Series. Philadelphia: SIAM; 2006. Vol. 2.

[6] Dang C, Nghiem L, Chen Z, Nguyen QP. Modeling Low Salinity Waterflooding: Ion Exchange, Geochemistry and Wettability Alteration. Paper SPE 166447 presented at the 2013 SPE Annual Technical Conference and Exhibition. 2013. New Orleans, LA, USA, 30 September – 2 October.

[7] Dang C, Nghiem L, Nguyen N, Chen Z. New Insights into the Critical Role of Geology in Modeling and Prediction of Low Salinity Waterflooding. Paper SPE 174294 presented at the SPE EUROPEC. 2015. Madrid, Spain, 1-4 June.

[8] Dang C, Nghiem L, Nguyen N, Chen Z, Nguyen Q. Evaluation of CO_2 low salinity water-alternating-gas for enhanced oil recovery. J Nat Gas Sci Eng 2016;35(2016):237–58.

[9] Dang C, Nghiem L, Nguyen N, Chen Z, Nguyen Q. Mechanistic modeling of low salinity water flooding. J Petrol Sci Eng 2016;146(2016):191–209.

[10] Dang C, Nghiem L, Nguyen N, Chen Z, Yang C, Bae W. A Comprehensive Evaluation of Alkaline Surfactant Polymer Flooding and Hybrid Process for Enhanced Oil Recovery. Paper SPE 187132 presented at the SPE Annual Technical Conference and Exhibition. 2017. San Antonio, TX, USA, 9-11 October.

[11] Dang C, Nghiem L, Nguyen N, Chen Z, Yang C, Nguyen Q. A framework for assisted history matching and robust optimization of low salinity waterflooding under geological uncertainties. J Petrol Sci Eng 2017;152(2017):330–52.

[12] Delshad M, Han C, Veedu FK, Pope AG. A simplified model for simulations of

alkaline-surfactant-polymer floods. J Petrol Sci Eng 2013;108(2013):1–9.
[13] Evje S, Hiorth A. A model for interpretation of brine dependent spontaneous imbibition experiments. Adv Water Resour 2010;34(2011):1627–42.
[14] Farajzadeh R, Matsuura T, Batenburg D, Dijk. Detailed Modeling of Alkali/Surfactant/Polymer (ASP) Process by Coupling a Multipurpose Reservoir Simulator to the Chemistry Package PHREEQC. SPE Reservoir Eval Eng 2012;15(04):423–35.
[15] Fernandes B, Pope G, Sepehrnoori K, Lashgari R. Advances in Chemical EOR Technologies: New Development in Field-Scale Chemical Flooding Simulation. Paper OTC-29287 presented at the Offshore Technology Conference. 2019. Houston, TX, USA, 6-9 May.
[16] Fjelde I, Asen SV, Omekeh A. Low Salinity Water Flooding Experiments and Interpretation by Simulations. Paper SPE 154142 presented at the Eighteenth SPE Improved Oil Recovery Symposium. 2012. Tulsa, OK, USA, April 14-18.
[17] Glover CJ, Puerto MC, Maerker JM, Sandvik EL. Surfactant Phase Behavior and Retention in Porous Media. SPE J 1979;19(3):183–93.
[18] Hamon G. Low Salinity Waterflooding: Facts, Inconsistencies and the Way Forward. Petrophysics 2016;57(1):41–50.
[19] Hirasaki GJ, Domselaar HR, Nelson RC. Evaluation of Salinity Gradient Concept in Surfactant Flooding. SPE J 1983;23(03):486–500.
[20] Huh C. Interfacial tensions and solubilizing ability of microemulsion phase that coexists with oil and brine. J Colloid Interface Sci 1979;71(1979):408–26.
[21] Jerauld GR, Lin CY, Webb KJ, Seccombe JC. Modeling Low Salinity Waterflooding. SPE Reservoir Eng 2008;11(6):1000–12.
[22] Johannessen AM, Spildo K. Enhanced Oil Recovery by Combining Surfactant with Low Salinity Injection. Energy Fuels 2013;2013(27):5738–49.
[23] Johannessen AM, Spildo K. Can Lowering the Injection Brine Salinity Further Increase Oil Recovery by Surfactant Injection under Otherwise Similar Conditions? Energy Fuels 2014;2014(28):6723–34.
[24] Jong S, Nguyen NM, Erbele CM, Nghiem LX, Nguyen QP. Low Tension Gas Flooding as a Novel EOR Method: An Experimental and Theoretical Investigation. Paper SPE 179559, SPE Improved Oil Recovery Conference. 2016. Tulsa, Oklahoma, USA, 11-13 April 2016.
[25] Khanamiri H, Torsater O, Stensen JA. Experimental Study of Low Salinity and Optimal Salinity Surfactant Injection. Paper SPE 174367 presented at the SPE EUROPEC. 2015. Madrid, Spain, 1-4 June.
[26] Khorsandi S, Qiao Changhe, Johns RT. Robust Geochemical Simulation of Alkali/Surfactant/Polymer Flooding with an Equation of State. Paper SPE-182656 presented at the SPE Reservoir Simulation Conference. 2017. Montgomery, TX, USA, 20-22 February.
[27] Korrani A, Sepehrnoori K, Delshad M. A Mechanistic Integrated Geochemical and Chemical-Flooding Tool for Alkaline/Surfactant/Polymer Floods. SPE J 2016;21(01):32–54.
[28] Korrani AKN. Mechanistic Modeling of Low Salinity Water Injection (PhD Dissertation) University of Texas at Austin; 2014.
[29] Korrani AKN, Jerauld G. Modeling Wettability Change in Sandstone and Carbonates Using a Surface-Complexation-Based Method. Paper SPE 190236 presented at the SPE Improved Oil Recovery Conference. 2018. Tulsa, OK, USA, 14-18 April.
[30] Kulkarni MM, Rao DN. Experimental Investigation of Miscible and Immiscible WAG Process Performance. J Petrol Sci Eng 2005;48(2005):1–20.
[31] Li Y, Huang C, Ding L, Li Z, Pan Y, Gao X. Deep Learning in Bioinformatics: Introduction, Application, and Perspective in Big Data Era. Methods 2019. https://doi.org/10.1016/j.ymeth.2019.04.008.
[32] Li Y, Zhang T, Sun S. Acceleration of the NVT Flash Calculation for Multicomponent Mixtures Using Deep Neural Network Models. Ind. Eng. Chem. Res. 2019;58(27):12312–22.
[33] Li Y, Zhang T, Sun S, Gao X. Accelerating Flash Calculation Through Deep Learning Methods. J Comput Phys 2019;394(2019):153–65.
[34] Li H, Yang C, Mirzabozorg A, Fedutenko E, Nghiem L. Using Multiple Objective Optimization for SAGD Simulation Numerical Tuning. Paper SPE 170024 presented at the SPE Heavy Oil Conference. 2014. Calgary, AB, Canada, 10-12 June.
[35] Luo H, Al-Shalabim EW, Delshad M, Panthi K, Sepehrnoori K. A Robust Geochemical Simulator to Model Improved Oil Recovery Methods. Paper SPE 173211 presented at SPE Reservoir Simulation Symposium. 2015. Houston, Texas, USA, 23-25 February.
[36] Mirzabozorg A, Nghiem L, Chen Z, Yang C, Li H. How Does the Incorporation of Engineering Knowledge Using Fuzzy Logic during History Matching Impact Reservoir Performance Prediction? Paper SPE 170011 presented at the SPE Heavy Oil Conference. 2014. Calgary, AB, Canada, 10-12 June.
[37] Mohammadi H. Mechanistic Modeling, Design, and Optimization of Alkaline/Surfactant/Polymer Flooding (PhD Dissertation) The University of Texas at Austin; 2008.
[38] Morrow NR, Buckley JS. Improved Oil Recovery by Low-Salinity Waterflooding. JPT, Distinguished Author Series 2011:106–12.
[39] Nghiem L, Skoreyko F, Gorucu E, Dang C, Shrivastava V. A Framework for Mechanistic Modeling of Alkali-Surfactant-Polymer Process in an Equation-of-State Compositional Simulator. Paper SPE 182628 presented at the SPE Reservoir Simulation Conference. 2017. Montgomery, Texas, USA, 20-22 February.
[40] Nghiem LX, Sammon P, Grabenstetter J, Ohkuma H. Modeling CO_2 Storage in Aquifers with Fully-Coupled Geochemical EOS Compositional Simulator. Paper SPE 89474 presented at the SPE Fourteenth Symposium on Improved Oil Recovery. 2004. Tulsa, OK, USA, April 17-21.
[41] Qiao C, Khorsandi S, Johns RT. A General Purpose Reservoir Simulation Framework for Multiphase Multicomponent Reactive Fluids. Paper SPE 182715 presented at the SPE Reservoir Simulation Conference. 2017. Montgomery, TX, USA, 20-22 February.
[42] Rivet SM, Lake LW, Pope GA. A Coreflood Investigation of Low Salinity Enhanced Oil Recovery. Paper SPE 134297 presented at the SPE ATCE. 2010. Florence, Italy, 19-22 September.
[43] Shehata AM, Kumar HT, Nasr-El-Din HA. New Insights on Relative Permeability and Initial Water Saturation Effects During Low Salinity Waterflooding for Sandstone Reservoirs. Paper SPE-180874 presented at the SPE Trinidad and Tobago Conference, Port of Spain, Trinidad and Tobago. 2016. Port of Spain, Trinidad and Tobago, June 13-15.
[44] Sheng JJ. Modern Chemical Enhanced Oil Recovery – Theory and Practice. Elsevier; 2011.
[45] Skauge A, Ghorbani Z, Delshad M. 2011. Simulation of Combined Low Salinity Brine and Surfactant Flooding. Paper B26 presented at the 16th European Symposium on Improved Oil Recovery, Cambridge, UK, 12-14 April.
[46] Sorop TG, Masalmeh SK, Suijkerbuijk BM, Van Der Line HA, Mahani H, Marcelis FA, et al. Relative Permeability Measurements to Quantify the Low Salinity Flooding Effect at Field Scale. Paper SPE 177856 presented at the Abu Dhabi International Petroleum Exhibition and Conference. 2015. Abu Dhabi, UAE, 9 – 12 November.
[47] Spildo K, Sun L, Djurhuus K, Skauge A. A Strategy for Low Cost, Effective Surfactant Injection. J Petrol Sci Eng 2014;117(2018):8–14.
[48] Tavassoli S, Korrani KZ, Pope GA, Sepehrnoori K. Low-Salinity Surfactant Flooding – A Multimechanistic Enhanced-Oil-Recovery Method. JPE Journal 2016;21(3):744–60.
[49] Teklu TW, Alameri W, Kazemi H, Graves R, AlSumaiti A. Low Salinity Water Surfactant CO_2 Enhanced Oil Recovery: Theory and Experiments. Paper B10 presented at the 18th European Symposium on Improved Oil Recovery. 2015. Dresden, Germany, 14-16 April.
[50] Webb KJ, Lager A, Black CJJ. Comparison of High/Low Salinity Water/Oil Relative Permeability. Presented at the International Symposium of the Society of Core Analysts, Abu Dhabi, UAE. 2008. 29 October – 2 November.
[51] Wei L. Interplay of Capillary, Convective Mixing and Geochemical Reactions for Long Term CO2 Storage in Carbonate Aquifers. First Break 2011;29(1).
[52] Wei L. Sequential coupling of geochemical reactions with reservoir simulations for waterflood and EOR studies. SPE J 2012;17(2):469–84.
[53] Yang C, Nghiem L, Erdle J, Moinfar A, Fedutenko E, Li H, et al. An Efficient and Practical Workflow for Probabilistic Forecasting of Brown Fields Constrained by Historical Data. Paper SPE-175122 presented at the SPE ATCE. 2015. Houston, TX, USA, 28-30 September.